Staven report
6.07.3.

Faculty of Civil Engineering and Geosciences
Section of Structural and Building Engineering
Steel and Timber Structures

Overall Buckling Behaviour of High Strength and Very High Strength Steel Columns

Gang Shi, Frans S. K. Bijlaard
(g.shi@tudelft.nl) (f.s.k.bijlaard@citg.tudelft.nl)

Steel and Timber Structures, Section of Structural and Building Engineering,
Faculty of Civil Engineering and Geosciences, Delft University of Technology
PO Box 5048, 2600 GA Delft, The Netherlands

Abstract:

This report mainly includes two parts. The first part is the finite element analysis on the overall buckling behaviour of welded box section and I-sections high strength (690MPa) steel columns under axial compression, which has been validated by the test results. The second part is the strong axis buckling tests of I-section high strength and very high strength (690MPa and 960MPa) steel columns with end restraints.

1 Introduction

Since the first application of steel in steel structures in the 19th century the development of steel construction has been closely linked to the development in material properties and production methods. Significant achievements concerning strength, economy, design versatility, fabrication and erection techniques and service performance would not have been possible without the substantial improvements of steel. Especially with the application of "new" production processes for carbon steels such as the thermo-mechanical rolling and the quenching and tempering process, steel with a high construction strength but guaranteeing also good fabrication properties such as weldability was introduced into the construction market [1].

It was established from analytic modelling and testing that the strength of columns fabricated from high strength steel exceeded the strength of columns of equal length and cross-section fabricated from ordinary steel when compared on a nondimensional basis [2]. The difference arose because the effects of imperfections such as out-of-straightness and residual stresses are less severe for high strength steel [1].

The ratios of residual stress at critical points in the cross-section to the yield stress were less for high strength steel columns than for ordinary steel columns, and it was shown that it was the ratio of residual stress to the yield stress, rather than the magnitude of residual stress itself, which governed the reduction in strength. The ratio was lower for high strength steel because the magnitude of residual stress was largely independent of the yield stress [2]. A method to take the increase in the relative resistance into account has been proposed [3] in which the imperfection factor is reduced with the yield strength according to

$$\alpha = \alpha_0 (235/f_y)^{0.8} \quad (1)$$

Here α_0 is the values of α in Eurocode 3 [4]. The first proposal was to put n=0.8, but it was later modified to n=1.0. This proposal was based on studies with steel yield stress up to 430MPa. It is likely to be applicable to higher grades but this remains to be proven by further research [1].

The effect of bow imperfection can easily be demonstrated by a calculation of resistance according to elastic theory. The result of such a calculation for buckling in the strong direction of an H-profile with bow imperfection *l*/1000 and no residual stresses has indicated that the relative resistance is higher for a higher yield strength [1].

Compared to ordinary steel, application of high strength steel in steel structures has the following advantages:

- Economy: By increasing the steel strength, the steel member section size and the structure weight can be reduced as well as the corresponding welding work and the welding material amount, also the coating material (fireproof, anticorrosive etc) and its work. And this could also reduce the cost of fabrication, conveyance and erection. Smaller structural sections can make larger net space for use. Especially the steel plate thickness will be decreased and then the weld size will be reduced, which can improve the weld quality and grade and increase the fatigue life of steel structures.
- Environment: Structures with less steel, welding and coating materials means less consumption of our world's scarce iron ore and other non-renewable resources. And it can also reduce the destruction to environment in the course of mining.
- Energy: Construction of less steel, welding and coating materials further means less consumption of energy to produce them, which is very important to us as our world faces the energy crisis.
- Safety: Modern high strength steel grades exhibit not only high strength values. Special grades combine this strength with excellent toughness so that a high safety both in fabrication and application of the structures is ensured. In particular, modern offshore steel grades performing at some of the lowest service temperatures are a good example [1].

For the research about high and very high strength steel structures, some studies have been done or are being implemented now. Girão Coelho etc applied S690 steel to the end-plate of end-plate connections [5]. Gustafsson did the experimental fatigue research for 550MPa steel welded connections [6]. Olsson etc analyzed the profitability of high strength steels in fatigue loaded structures [7]. Nishino [8], Rasmussen [9], McDermott [10] and Clarin [11] etc investigated the local buckling behaviour of high strength steel columns by tests and analysis. Beg etc implemented experimental and nonlinear numerical analysis of the local stability of welded I beams made of high strength steel [12]. Abspoel and Pijpers are studying the local buckling of high strength steel plate girders and the suitability of high strength steel for structural application based on assessment of weldability and mechanical performance respectively [13].

About the overall stability of high and very high strength steel columns, there are only a few experimental researches which only cover two types of sections such as welded box and welded I-section (flame-cut flange and about weak axis), single steel grade (690MPa) [2][8][14].

For the application of high and very high strength steel structures, there have already been some projects.

The roof truss structure of the Sony Centre (Fig. 1) in Berlin, Germany, is made of steel grade S460 and S690. High strength steel was used to keep the dimensions of the cross sections small that were provided with an envelope for fire protection [1].

The first Japanese project using high strength steel in structural elements of a building is the Landmark Tower in central Yokohama (Fig. 2). Completed in 1989, it used steel with a minimum tensile strength of 600 MPa in the I-section columns fabricated from plates made with the thermomechanical process [15].

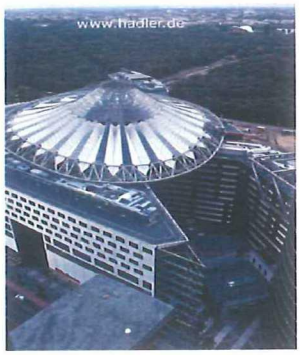

Fig. 1. Sony Centre in Berlin, Germany

Fig. 2. Landmark Tower in Yokohama, Japan

The Star City Complex (Fig. 3) in Sydney, Australia, applied 650MPa and 690MPa high strength steels in two areas. The first area is the basement columns and column section sizes were reduced. The local council had already specified that this building was to provide a minimum of 2500 spaces. This in turn forced the architect to restrict the column sizes in the underground car park areas to 500mm wide and therefore the only solution was to use high strength steel in a composite column arrangement. The other area was the roof trusses to the Lyric Theatre. There were two main trusses supporting the roof, each truss being 3.5m deep and covering a span of 30m. It was in the tension elements being subjected to the highest forces that the high strength steel was used (Fig. 4) [15].

Fig. 3. Star City in Sydney, Australia

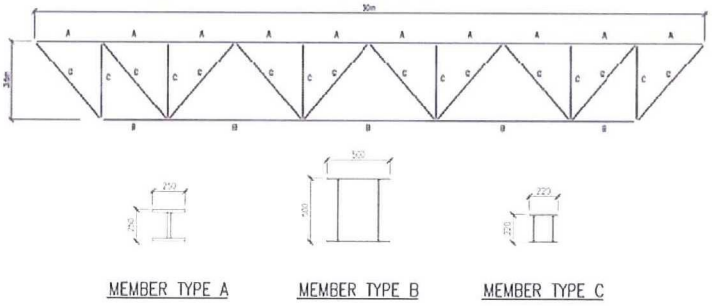

Fig. 4. Star City truss elevation and member sections

The Latitude in Sydney (Fig. 5), completed in 2005, is 55 storeys high. In this project, a large, steel transfer structure, 7m deep, transferred loads from the new columns onto the existing concrete and also created a flat construction platform for work above the 16th floor. 16mm thick 690MPa steel plates were used to reduce the weight of the transfer. Although the amount of high strength steel used was only 280t (<5%), the advantages which resulted were impressive [15].

High strength steel has also been applied in many bridges. A few examples are following.

In the Rhine bridge Dusseldorf-Ilverich (Fig. 6), a cable-stayed road bridge, the V-shaped pylons are made of S460 steel to keep the height of the towers small, to minimize plate thickness to keep the weld volume for butt welds small and to avoid preheating in order to reduce the welding cost [1].

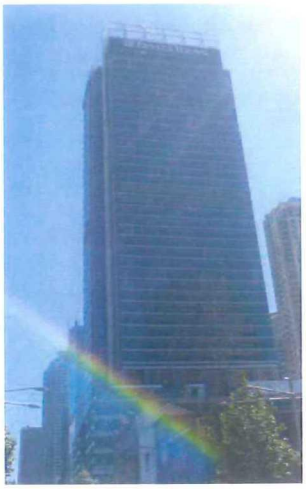

Fig. 5. Latitude in Sydney, Australia

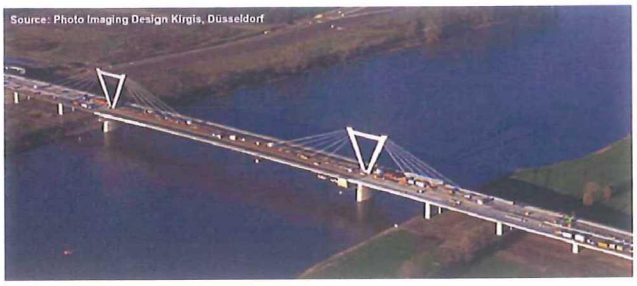

Fig. 6. Rhine bridge Dusseldorf-Ilverich

In Millau Viaduct bridge in France, S460 steel plates with thicknesses up to 80mm have been applied for the entire central box and some connecting elements in order to resist high loads without increasing the amount of steel used, reduce cantilever bending moments during launching of the bridge, apply a more efficient welding process and reduce transport weights from the workshop to the site [1].

Fig. 7. Millau Viaduct bridge in France

Fast Bridge 48 is a 48m single-span bridge system for loads up to Military Class 70 (MLC 70, approximately 64 metric tonnes) according to North Atlantic Treaty Organization (NATO) standards. It is made of extra high strength steels (S960 and S1100) and can be deployed in less than 90 minutes and retrieved in the same time from either side of a river or dry gap [1].

2 Residual Stress

2.1 Welded box section

Rasmussen *et al* [2] measured the residual stress of the 690MPa steel square box section, as shown in Fig. 8, with b=90mm, t=5mm. The measured steel yield stress in tension f_y is 705MPa. The specimen was fabricated by manual Gas Metal Arc Welding (GMAW). The steel plates were guillotined into strips. The strips were tack-welded into sections before final welding. And the steel plates were welded at ambient temperature. A single run of

weld was laid along each fillet so that four runs were laid for the section. The residual strains were measured using strain gauges. The residual stress measurements are shown in Table 1, in which the maximal amount (σ_r=-148MPa) is $0.21f_y$.

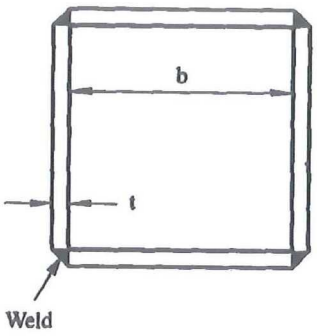

Fig. 8. Box section of Rasmussen *et al*

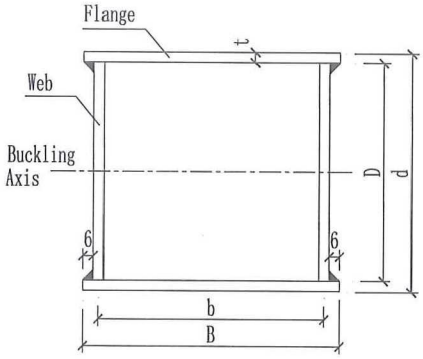

Fig. 9. Box section of Usami *et al*

Table 1 Residual stress of box section

	Residual stress (MPa)
Side 1	-145
Side 2	-92
Side 3	-148
Side 4	-105

When studying the plate slenderness limits for high strength steel sections, Rasmussen *et al* [9] measured the residual stresses of another 3 square box sections fabricated by 690MPa steel, as shown in Fig. 8 and Table 2.

Table 2 Dimensions of specimens of Rasmussen *et al*

Specimen	b (mm)	t (mm)	b/t	Residual stress (MPa)					σ_r/f_y
				Side 1	Side 2	Side 3	Side 4	Average σ_r	
B1RS	80	5	16	-163	-112	-174	-227	-169	0.252
B2RS	110	5	22	-125	-135	-112	-84	-114	0.170
B3RS	140	5	28	-64	-78	-	-78	-73	0.109

Usami *et al* [14] measured the residual stress of three 690MPa steel square box sections, shown in Fig. 9 and Table 3. Measured residual stress patterns were all similar in shape to the well-known pattern, i.e., nearly constant compressive stresses were observed over the central portion of each plate and rather high tensile stresses (about 60% of the yield stress) were measured near the flange-web junctions. The average value of measured compressive

residual stresses, f_{rc}, in each specimen were 13.8%, 8.7% and 11.2% of the yield stress for specimens RES-22, RES-33 and RES-44, respectively. Thus, residual compressive stresses of about $0.1f_y$ are supposed to be locked in all test specimens.

Table 3 Dimensions of specimens of Usami *et al*

Specimen	B(mm)	D(mm)	t(mm)	b/t
RES-22	150	126	6	22
RES-33	216	192	6	33
RES-44	282	258	6	44

Nishino *et al* [8] measured the residual stress of 2 welded square box sections fabricated from A514 (nominal yield stress 690MPa) steel with flame-cut plates, shown in Table 4. The welding details are given in Fig. 10. After small tack welds were deposited to fix the shape, submerged arc welding was employed throughout the fabrication. The residual stress distributions were in Fig. 11 and Table 5. The residual stress patterns show tensile residual stress at the weld metal and its nearby area and its magnitude was slightly below the yield stress. Compressive residual stresses distributed over the rest of the cross section and the magnitudes were larger for the small cross sections than for the large cross sections due to equilibrium requirements.

Table 4 Dimensions of specimens of Nishino *et al*

Specimen	b(in)	t(in)	b/t
T-1	11.2	0.255	44.0
T-2	6.77	0.258	26.2

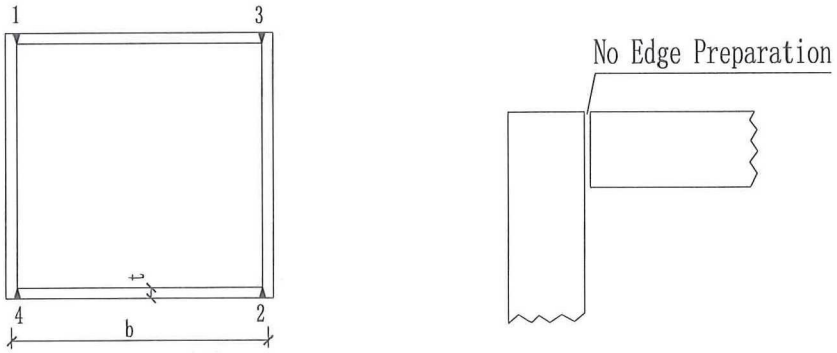

Nos. 1 to 4 refer to welding sequence

Fig. 10. Box section of Nishino *et al*

Table 5 Average values of compressive residual stress

Specimen	Yield strength f_y (ksi)	Average compressive residual stress σ_{rc} (ksi)	σ_{rc}/f_y
T-1	116	11~12	0.10
T-2	104	14~15	0.15

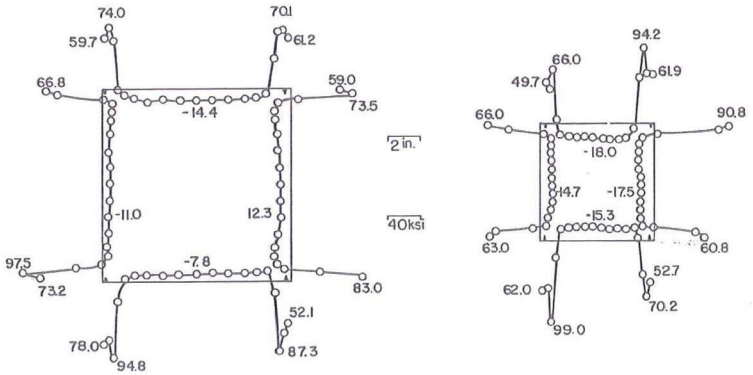

T-1 T-2

Fig. 11. Residual stress distribution (unit: ksi; 1ksi=6.895MPa)

2.2 Welded I-section

Rasmussen *et al* [2] measured the residual stress of the 650MPa steel I-section with flame-cut flanges, as shown in Fig. 12 and Table 6. The measured steel yield stress in tension f_y is 660MPa. The specimen was fabricated by manual Gas Metal Arc Welding (GMAW). The steel plates were flame-cut into strips. The strips were tack-welded into sections before final welding. A preheat of 50℃ was used. A single run of weld was laid along each fillet so that four runs were laid for the section. The residual strains were obtained using the sectioning technique. The residual stresses measured are shown in Fig. 13. The figure also shows the average of the compressive residual stress measurements in the web (σ_{rw}) and in the flanges (σ_{rf}), which are $0.048f_y$ and $0.205f_y$ respectively, assumed to be positive as tensile. The calculation of the average compressive residual stress in the flanges (σ_{rf}) did not include the measurements closest to the free edges of the flanges, since these measurements were tensile because the virgin plates were flame-cut into strips.

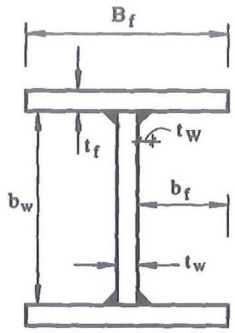

Fig. 12. I-section of Rasmussen *et al*

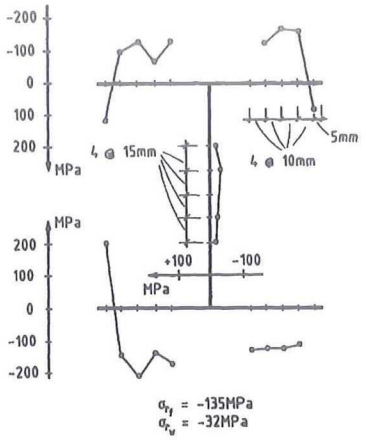

Fig. 13. Residual stresses of welded I-section with flame-cut flanges

Table 6 Dimensions of I-sections with flame-cut flanges from Rasmussen *et al* (mm)

B_f	b_f	t_f	b_w	t_w	B_f/t_f	b_w/t_w
140	66	8	140	8	17.5	17.5

Rasmussen *et al* [9] also measured the residual stress of the 650MPa steel I-section with guillotined flanges, as shown in Fig. 12 and Table 7. The measured steel yield stress in tension f_y is 725MPa. The residual stresses measured are shown in Fig. 14 and Table 7. The figure also shows the average of the compressive residual stress measurements in the web (σ_{rw}) and in the flanges (σ_{rf}). The calculation of the average compressive residual stress in the flanges (σ_{rf}) did not include the four measurements closest to the welds, since these measurements were taken in the transition zones between the tension blocks at the welds and the compression blocks away from the welds.

Table 7 I-sections with guillotined flanges from Rasmussen *et al* (mm)

Specimen	B_f	b_f	t_f	b_w	t_w	B_f/t_f	b_w/t_w	σ_{rw} (MPa)	σ_{rf} (MPa)	σ_{rw}/f_y	σ_{rf}/f_y
I1RS	96	45	6	120	6	16.0	20	-100	-153	0.138	0.211
I2RS	116	55	6	150	6	19.3	25	-76	-124	0.105	0.171
I3RS	136	65	6	180	6	22.7	30	-69	-146	0.095	0.201

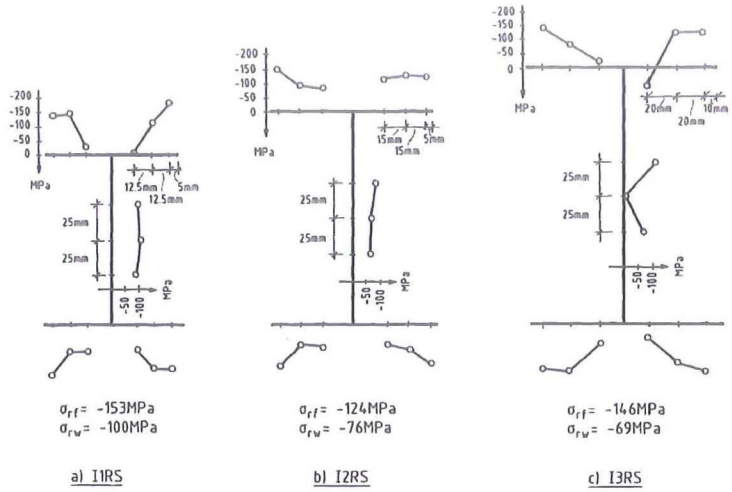

Fig. 14. Residual stresses of welded I-section with guillotined flanges

Beg *et al* [16] measured the residual stress of the 700MPa steel I-section, as shown in Fig. 15. The MAG welding process using the flux-cored electrode FILTUB 32B (1.4 mm diam., f_y=690MPa) and preheating to 150-175°C was applied. The average value of compressive residual stresses for cross-section B amounted to 73MPa ($0.09f_y$), and for cross-section D it was 123MPa ($0.14f_y$), where the average compressive residual stresses in flanges amounted to approximately 100MPa ($0.18f_y$). For cross-sections B and D, b=270mm and 220mm, which means b/t=22.5 and 18.3 respectively.

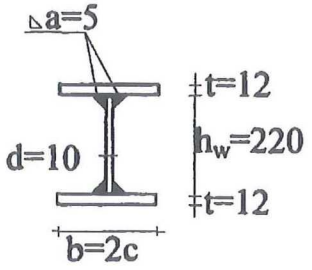

Fig. 15. I-section of Beg *et al*

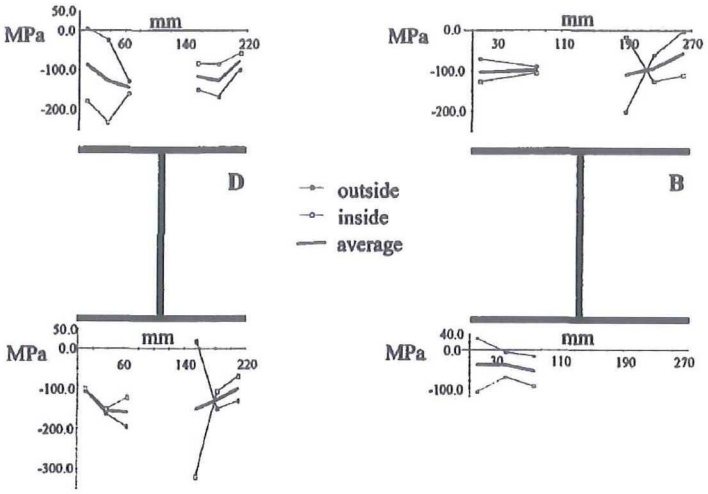

Fig. 16. Residual stresses of I-section of Beg *et al*

2.3 Welded cruciform section

Rasmussen *et al* [9] also measured the residual stress of the 650MPa steel I-section with guillotined flanges, as shown in Fig. 17 and Table 8. The measured steel yield stress in tension f_y is 725MPa. The residual stresses measured are shown in Fig. 18 and Table 8. The

figure also shows the average of the compressive residual stress measurements in the web (σ_{rw}) and in the flanges (σ_{rf}). The calculation of the average compressive residual stress in the flanges (σ_{rf}) did not include the four measurements closest to the welds, since these measurements were taken in the transition zones between the tension blocks at the welds and the compression blocks away from the welds.

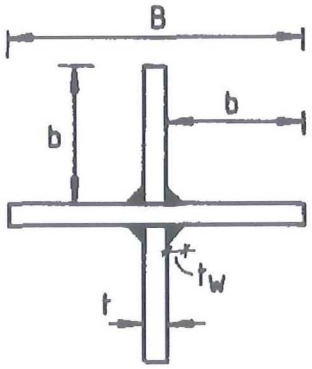

Fig. 17. Cruciform section of Rasmussen *et al*

Table 8 Cruciform sections with guillotined flanges from Rasmussen *et al* (mm)

Specimen	B	b	t	b/t	σ_r (MPa)	σ_r/f_y
X1RS	86	40	6	6.7	-127	0.175
X2RS	116	55	6	9.2	-109	0.150
X3RS	146	70	6	11.7	-87	0.120

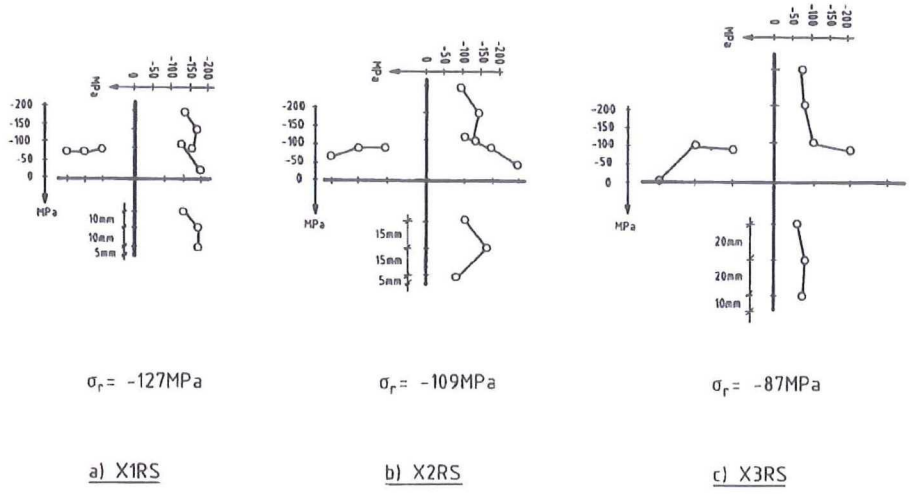

Fig. 18. Residual stresses of cruciform sections

3 Verification of Finite Element Analysis (FEA)

In order to use the finite element analysis to analyze the overall buckling behaviour of high strength pin-ended steel columns under axial compression, firstly, 16 test specimens from other literatures, including 11 square and rectangular welded box sections and 5 welded I-sections, have been calculated by the large-scale general-purpose finite-element software, ANSYS, to verify the finite element models by the test results.

3.1 Test specimens for FEA

3 groups of test specimens collected from other literatures are calculated. Specimens of group 1 are 650MPa welded box sections as shown in Fig. 8 and Table 9 [2], in which, L is the pin-ended column length, A is the section area, I is the second moment of area, r is the radius of gyration, e is the total geometrical initial imperfection of the centroid at mid-length, which is equal to v_0+e_0, and v_0 is the deviation of the column axis at mid-length from a straight line connecting the ends, and e_0 is the eccentricity of the applied load at the supports, as shown in Fig. 19.

Table 9 Specimens of group 1

Specimen	b (mm)	t (mm)	L (mm)	A (mm^2)	I (mm^4)	r (mm)	$e/L\times10^3$
Nominal	90	5	-	1850	2.75×10^6	38.6	-
B1150C	88.9	5.00	1149	1828	2.64×10^6	38.0	0.43
B1950C	88.3	4.96	1950	1801	2.57×10^6	37.8	0.26
B3450C	90.2	4.97	3451	1843	2.74×10^6	38.6	0.12
B1150E	87.6	4.95	1150	1783	2.51×10^6	37.5	1.83
B1950E	89.4	4.97	1950	1827	2.67×10^6	38.2	1.64
B3450E	89.9	4.94	3451	1825	2.69×10^6	38.4	0.84

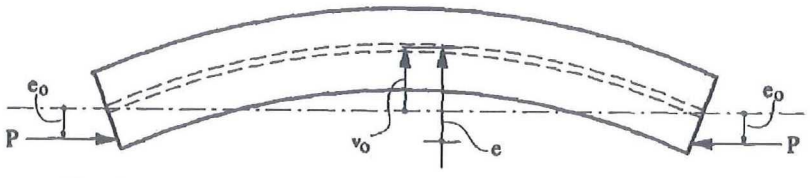

Fig. 19. Loading eccentricity and geometric imperfection

Specimens of group 2 are 690MPa welded square and rectangular box sections as shown in Fig. 9 and Table 10 [14], in which, A, L, r and e have the same definition with specimens of group 1.

Table 10 Specimens of group 2

Specimen	B (mm)	D (mm)	t (mm)	A (mm^2)	L (mm)	r (mm)	$e/L\times10^3$
S-35-22	151	127	6.00	3340	1880	54.9	0.629
S-50-22	151	122	6.01	3280	2690	53.1	0.315
R-50-22	151	94.2	6.00	2940	2090	42.9	0.397
R-65-22	151	94.4	6.01	2950	2720	42.9	0.242
ER-50-22	151	94.3	6.01	2950	2090	42.8	5.418

Specimens of group 3 are 690MPa welded I-sections with flame-cut flanges, as shown in Fig. 12 and Table 11 [2], in which, A, L, I, r and e have the same definition with specimens of group 1.

Table 11 Specimens of group 3

Specimen	B_f (mm)	b_f (mm)	t_f (mm)	b_w (mm)	t_w (mm)	tw (mm)	L (mm)	A (mm^2)	I (mm^4)	r (mm)	$e/L\times10^3$
Nominal	140.0	66.0	8.00	140.0	8.00	6.0	-	3430	3.66×10^6	32.7	
I1000C	141.5	66.9	7.70	140.0	7.70	6.0	1000	3329	3.64×10^6	33.1	0.70
I1650C	141.5	66.9	7.70	141.5	7.66	5.1	1649	3315	3.64×10^6	33.1	0.25
I1000E	141.1	66.7	7.67	141.8	7.71	6.8	1000	3350	3.60×10^6	32.8	1.30
I1650E	141.5	66.9	7.71	143.0	7.75	5.3	1649	3346	3.65×10^6	33.0	0.61
I2950E	140.3	66.3	7.75	142.0	7.74	6.2	2950	3351	3.57×10^6	32.6	0.68

3.2 Finite element model

In the finite element models, all the columns are meshed by 3-D Linear Finite Strain Beam Element BEAM188 and each column is meshed into 20 elements. BEAM188 can be used with any cross-section defined by the user. User defined sections for test specimens are shown in Fig. 20. For the specimens of group 1, each side of the square box section is meshed into 18 equal square divisions. For specimens in group 2, the flange is meshed into 25 equal square divisions, and the web is meshed into 15 and 21 divisions respectively for rectangular and square sections. For specimens in group 3, the flange is meshed into 23 equal square divisions, and the web is meshed into 12 divisions. In all the finite element models, welds are also simulated. The input files to define parameters for a typical specimen column (B1150E) model and to generate a typical specimen column (B1150E) section in ANSYS are in Annex 1 and Annex 2 respectively. A typical FEA model (B1150E) is shown in Fig. 21.

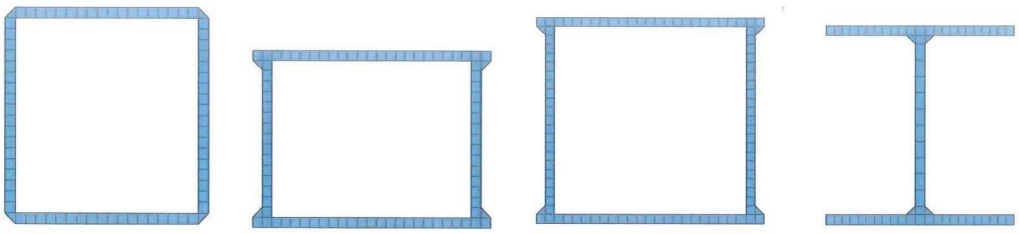

Group 1 | Rectangular section of group 2 | Square section of group 2 | Group 3

Fig. 20. Sections in FEA

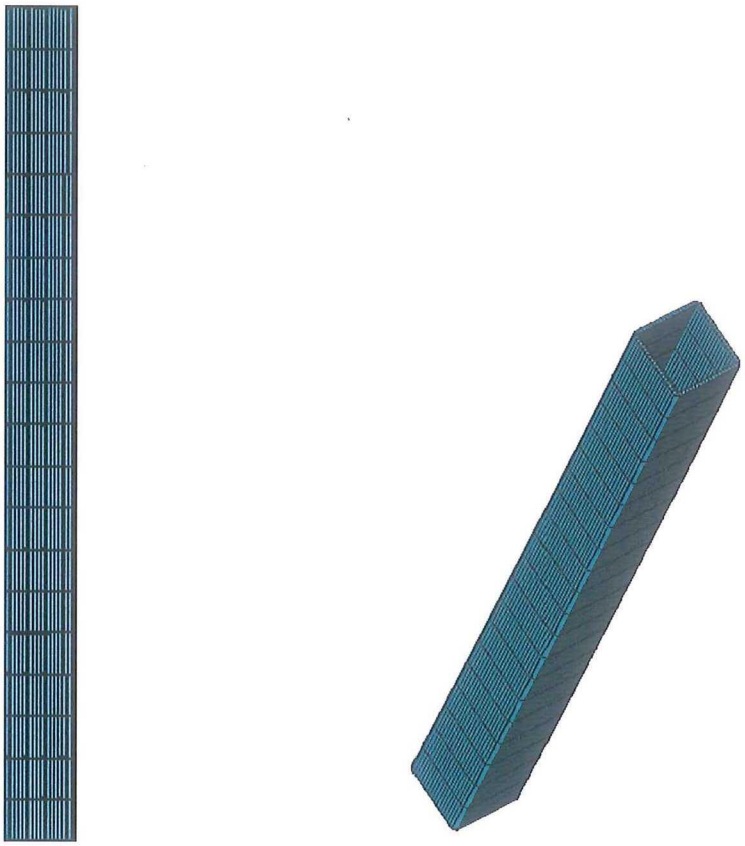

Fig. 21. A typical FEA model (B1150E)

In the finite element models, the adopted stress-strain relationships of steel are the multi-linear kinematic hardening model with von Mises yielding rule. The material properties for specimens of group 1 and 3 are shown in Fig. 22 and Table 12, and that for specimens of group 2 is shown in Fig. 23. All the material properties are from the material tests results. The Poisson's ratio is 0.3.

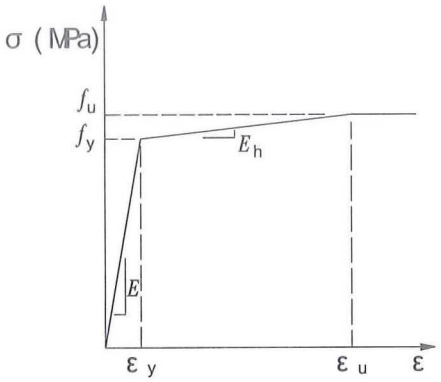

Fig. 22. Stress-strain relationship for specimens of group 1 and 3

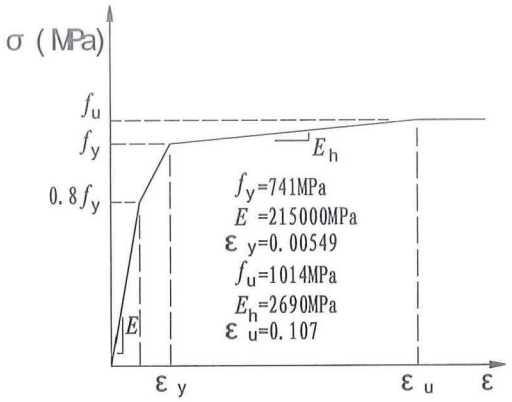

Fig. 23. Material properties for specimens of group 2

Table 12 Stress-strain relationships for specimens of group 1 and 3

Specimen	f_y (MPa)	ε_y	f_u (MPa)	ε_u
Group 1	705	0.0033	750	0.076
Group 3	660	0.0031	725	0.084

In all the FEA models, y axis is along the longitudinal direction of the specimen section center, x and z axes are the weak and strong axes of the specimen section respectively. For all the models, the x-direction displacement and the torsional deformation of all the nodes are restrained, the z-direction displacement on both ends and the y-direction displacement on the bottom end of all the specimens are restrained.

3.3 Analysis program

The analysis and solution of each specimen model includes 3 load steps, in which the analysis type is always "Large Displacement Static" to consider the P-□ effect. In the first step, the model of the specimen column without initial geometric imperfections or residual stress is created, then an axial force (y-direction) which is smaller than the yielding axial load of the column section is applied on the top end, and the solution is implemented to get the stiffness matrix of the model. In the second step, the eigenvalue buckling analysis is performed to get the overall Euler buckling mode of the column. In the third step, the residual stress is input as the initial stress on the column section, and the initial geometric imperfection, e, is imported with the first-order buckling mode shape and the magnitude at the column mid-height shown in Table 7, Table 8 and Table 9, then the axial force is applied on the top end and the arc-length method is adopted to get the column loading capacity. The main input file to do the FEA of a typical specimen column (B1150E) is in Annex 3.

3.4 Residual stress in FEA models

The residual stress is applied on the column section as the initial stress. Firstly, the residual stress file for each specimen is created by the ANSYS order *VWRITE. The input file to create the residual stress file for a typical specimen column (B1150E) model is in Annex 4. Then the residual stress is applied at the element integration points of the column section by the ANSYS order ISFILE to read the residual stress file into the FEA model. In each division of the element shown in Fig. 20, there are 4 integration points, at which the applied residual stresses are identical. The distribution of the integration points and the division nodes of sections in Fig. 20 are shown in Annex 5, in which red dots are integration points and blue triangular points are division nodes of sections.

The applied residual stress distributions for the specimens of group 1, 2 and 3 are shown as red and blue lines in Fig. 24(a), Fig. 25(a) and Fig. 26(a) respectively. As it is regarded that the residual stresses are identical in each division of the section, the actually adopted residual stress distributions in FEA models are shown as red and blue lines in Fig. 24(b), Fig. 25(b) and Fig. 26(b) respectively. And all the parameters are listed in Table 13, Table 14, Table 15 and Table 16 respectively. All the residual stress distribution modes are symmetric about both the strong and weak axes of the section. During the FEA, 3 residual stress distribution modes have been applied for each specimen column in order to study the influence of the residual stress on its overall buckling behaviour. The standard residual stress distribution mode, RS-S, is from the tests results, RS+1 and RS-1 mean more and less residual stress respectively.

For group 1 specimens, the residual stress distributions are the same for all the four sides as in Fig. 24 and Table 13. For group 2 and 3 specimens, the residual stress of the welds is consistent with the column web, as blue lines in Fig. 25 and Fig. 26.

Table 13 Residual stress distribution for specimens of group 1

Mode	a(mm)	b(mm)	c(mm)	f_a	f_b	f_c
RS+1	5	5	70	f_y	$0.385f_y$	$-0.23f_y$
RS-S				$0.85f_y$	$0.325f_y$	$-0.2f_y$
RS-1				$0.8f_y$	$0.31f_y$	$-0.18f_y$

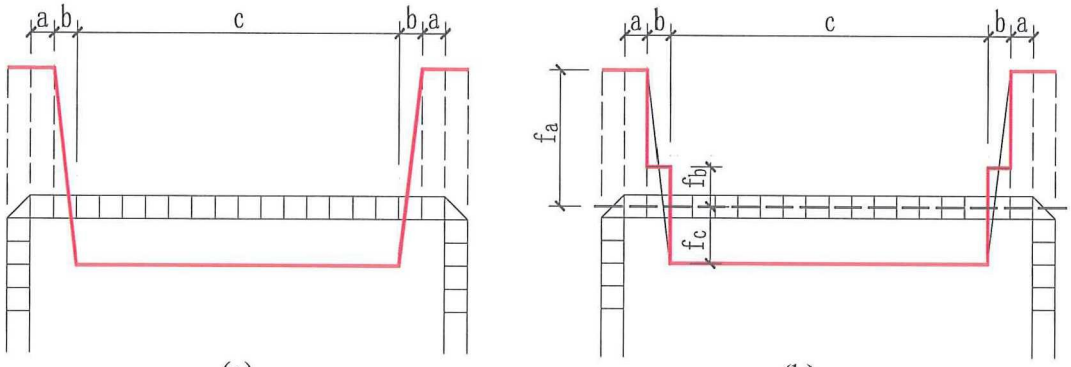

(a) (b)

Fig. 24. Residual stress distribution for specimens of group 1

Table 14 Residual stress distribution for rectangular section specimens of group 2

	a(mm)	b(mm)	c(mm)	d(mm)	e(mm)	f(mm)
	12	6	114	6	6.3	69.4
Mode	f_a	f_b	f_c	f_d	f_e	f_f
RS+1	$0.68f_y$	$0.245f_y$	$-0.19f_y$	$0.68f_y$	$0.245f_y$	$-0.19f_y$
RS-S	$0.5f_y$	$0.18f_y$	$-0.14f_y$	$0.5f_y$	$0.18f_y$	$-0.14f_y$
RS-1	$0.36f_y$	$0.13f_y$	$-0.1f_y$	$0.36f_y$	$0.13f_y$	$-0.1f_y$

Table 15 Residual stress distribution for square section specimens of group 2

	a(mm)	b(mm)	c(mm)	d(mm)	e(mm)	f(mm)
	12	6	114	6	6	102
Mode	f_a	f_b	f_c	f_d	f_e	f_f
RS+1	$0.8f_y$	$0.305f_y$	$-0.19f_y$	$0.8f_y$	$0.305f_y$	$-0.19f_y$
RS-S	$0.6f_y$	$0.23f_y$	$-0.14f_y$	$0.6f_y$	$0.23f_y$	$-0.14f_y$
RS-1	$0.42f_y$	$0.16f_y$	$-0.1f_y$	$0.42f_y$	$0.16f_y$	$-0.1f_y$

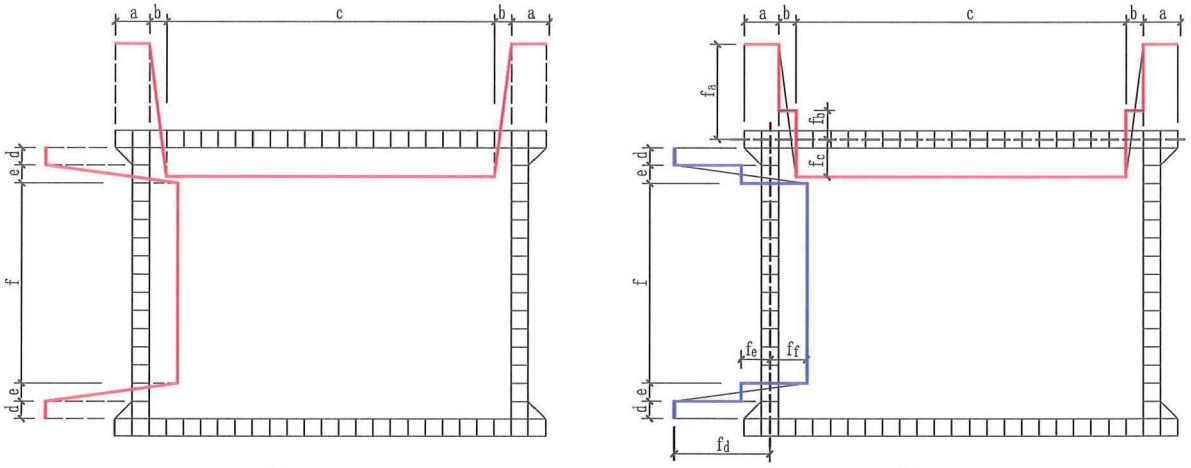

(a) (b)

Fig. 25. Residual stress distribution for specimens of group 2 including rectangular and square sections

Table 16 Residual stress distribution for specimens of group 3

Mode	a(mm)	b(mm)	c(mm)	d(mm)	e(mm)	f(mm)	g(mm)	h(mm)
RS+1	8	6	54	6	6	12.8	102.4	0
RS-S	8	6	54	6	6	12.8	102.4	0
RS-1	8	6	48	6	6	12.8	102.4	6
Mode	f_a	f_b	f_c	f_d	f_e	f_f	f_g	f_h
RS+1	f_y	$0.365f_y$	$-0.27f_y$	$0.065f_y$	f_y	$0.41f_y$	$-0.18f_y$	$0.4f_y$
RS-S	$0.8f_y$	$0.3f_y$	$-0.2f_y$	$0.15f_y$	$0.8f_y$	$0.325f_y$	$-0.15f_y$	$0.5f_y$
RS-1	$0.7f_y$	$0.24f_y$	$-0.22f_y$	$0.065f_y$	$0.7f_y$	$0.275f_y$	$-0.15f_y$	$0.35f_y$

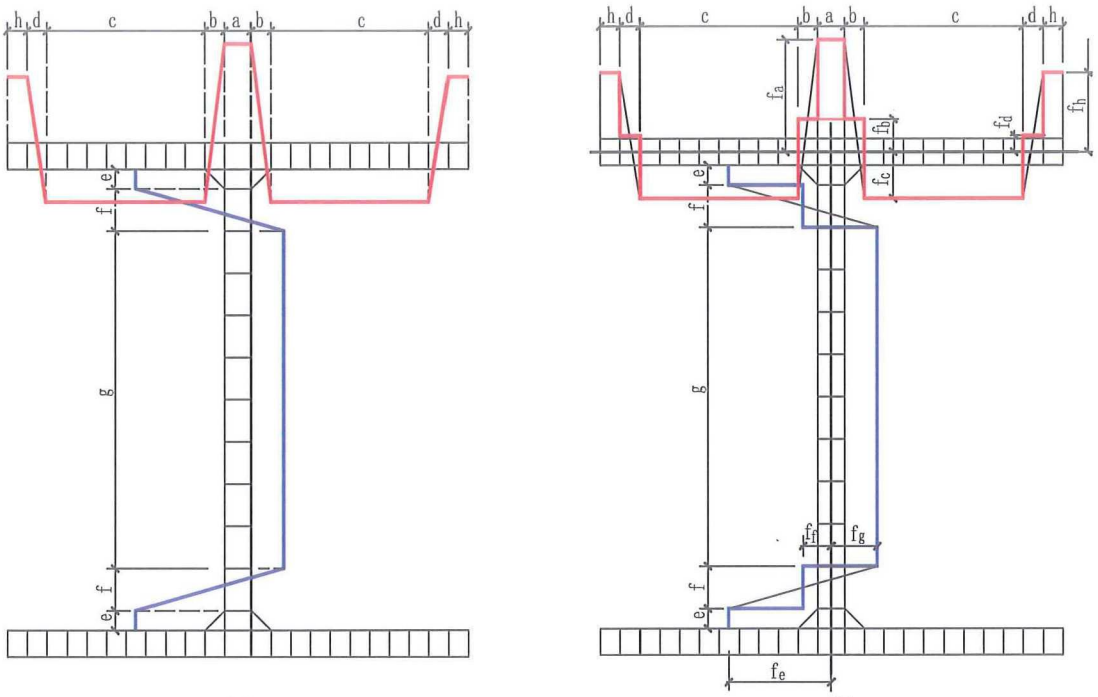

(a) (b)

Fig. 26. Residual stress distribution for specimens of group 3

3.5 FEA results

The ultimate deformation of a typical specimen (B1150E) is shown in Fig. 27. The FEA results and the comparison with the test results for all the specimens are listed in Table 17, Table 18 and Table 19, from which, it can be concluded that, by inputting the measured residual stress and geometric imperfections, the FEA results of the specimen loading capacities are almost the same with the test results, which validates that the finite element model applied is accurate enough to do the analysis on the buckling behaviour of high strength steel columns under axial compression.

And the influence of the residual stress variation on the overall buckling loading capacity of the high strength steel columns is not much.

3.6 The follow-up work

Next step, for high strength steel columns with box sections and I-sections, several typical section dimensions which can cover the regular dimensions in practical projects will be adopted. And the buckling behaviour of these columns under axial compression will be analyzed by the above validated finite element model. During FEA, the initial geometric imperfection with the shape of first-order Euler buckling mode and a central bow of l‰ length of the column. And then the buckling curves for box section and I-section (about the weak axis) high strength steel columns will be proposed.

Table 18 FEA results and comparison for specimens of group 2

Specimen	Loading capacity (kN)				RS+1 test	RS-S test	RS-1 test
	test	RS+1	RS-S	RS-1			
S-35-22	2112	2155.9	2157.4	2129.9	1.02	1.02	1.01
S-50-22	1798	1668.2	1738.3	1805.7	0.93	0.97	1.00
R-50-22	1622	1557.9	1606.0	1657.8	0.96	0.99	1.02
R-65-22	1299	1257.7	1332.2	1383.6	0.97	1.03	1.07
ER-50-22	1220	1206.0	1227.4	1235.9	0.99	1.01	1.01
Average					0.97	1.00	1.02
Standard deviation					0.03	0.02	0.02

Table 19 FEA results and comparison for specimens of group 3

Specimen	Loading capacity (kN)				RS+1 test	RS-S test	RS-1 test
	test	RS+1	RS-S	RS-1			
I1000C	2092	1805.0	1882.6	1957.2	0.86	0.90	0.94
I1650C	1751	1929.5	2023.6	2127.1	1.10	1.16	1.21
I1000E	2192	1778.2	1855.0	1915.4	0.81	0.85	0.87
I1650E	1682	1604.6	1680.3	1688.4	0.95	1.00	1.00
I2950E	745	770.7	786.6	789.9	1.03	1.06	1.06
Average					0.95	0.99	1.02
Standard deviation					0.12	0.12	0.13

4 Buckling Tests of High Strength and Very High Strength Steel Columns

For two aims, the strong axis buckling tests of 8 I-section high strength and very high strength steel columns with one beam connected on each end have been done.

The first aim is that, because until now there haven't been any available research results on the overall buckling behaviour of I-section high strength and very high strength steel columns about the strong axis, the tests are going to validate the FEA model for analyzing this behaviour. And then use this validated FEA model to do systematic study on the overall buckling behaviour of I-section high strength and very high strength steel columns about the strong axis.

The second aim is to investigate the influence of the column end restraints on its overall buckling behaviour.

4.1 Test specimens

8 specimens of I-section high strength and very high strength steel columns with one beam connected on each end have been designed as shown in Fig. 28, Table 20 and Table

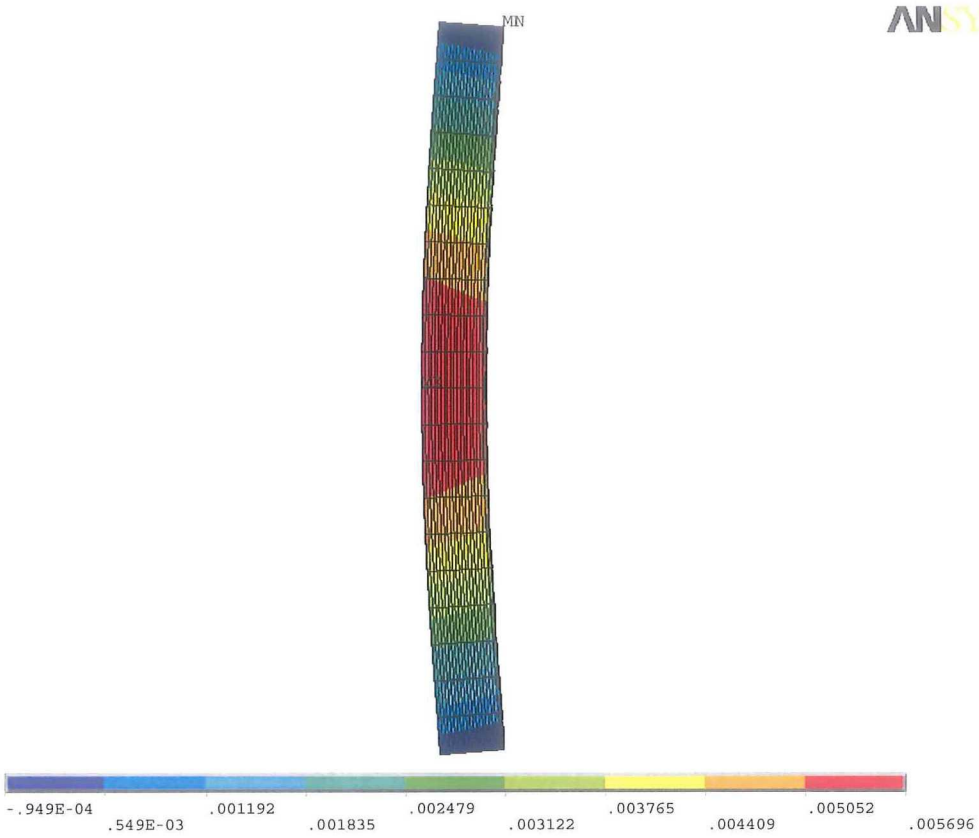

Fig. 27. Deformation of a typical specimen (B1150E)

Table 17 FEA results and comparison for specimens of group 1

Specimen	Loading capacity (kN)				RS+1 test	RS-S test	RS-1 test
	test	RS+1	RS-S	RS-1			
B1150C	1174	1140.8	1148.3	1158.3	~~0.97~~	~~0.98~~	~~0.99~~
B1950C	1078	935.4	972.3	986.8	0.87	0.90	0.92
B3450C	469	477.9	478.5	478.7	1.02	1.02	1.02
B1150E	1137	1049.0	1066.2	1074.1	0.92	0.94	0.94
B1950E	926	833.9	860.0	870.5	0.90	0.93	0.94
B3450E	438	437.2	443.0	443.8	1.00	1.01	1.01
Average					0.95	0.96	0.97
Standard deviation					0.06	0.05	0.04

21. In which, the specimen name includes 3 parts, the first number is the specimen serial number, the second number is the steel grade, and the third number is the column nominal length. λ is the nominal pin-ended column slenderness, i.e., L/r. $\overline{\lambda}$ is the real non-dimensional slenderness which considers the influence of the column end restraints on its buckling length, i.e., $\sqrt{\frac{Af_y}{N_{cr}}}$.

The distribution of non-dimensional slenderness for all the specimens is shown in Fig. 29. As in Eurocode 3 [4] the buckling curve b is adopted for welded I-sections about the strong axis when the plate thickness is not bigger than 40mm, the buckling curve b is also drawn in Fig. 29.

Table 20 Details of the test specimens

Specimen	h (mm)	b (mm)	t_w (mm)	t_f (mm)	t_e (mm)	L (mm)	Steel
1-690-1300	120	100	8	10	4	1300	S690
2-960-1300	90	80	6	8	3	1300	S960
3-690-2700	120	100	8	10	4	2700	S690
4-960-2700	120	100	8	10	4	2700	S960
5-690-3600	82	70	6	6	3	3600	S690
6-960-3600	96	80	6	8	3	3600	S960
7-690-3600	60	50	5	5	3	3600	S690
8-960-3600	60	60	6	6	3	3600	S960

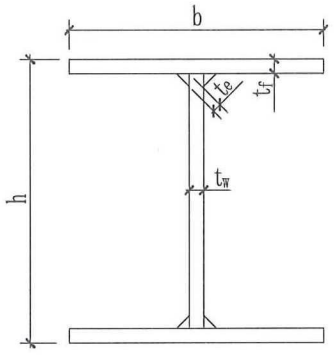

Fig. 28. Specimen sections

The test configuration is illustrated in Fig. 30. On both beam end supports load cells are used to measure the beam end reaction force. The displacements are measured by means of Linear Variable Displacement Transducers (DT). DT1, 2,4, 6 and 7 are to measure the column in-plane deformation. DT8 is to monitor the column mid-height out-of-plane deforma-

tion. DT9 is to measure the column top end axial compression deformation. DT10 and 11, DT12 and 13 are to measure the rotation on the column top and bottom ends respectively. DT3 and 5 are to monitor the column mid-height torsional deformation (Fig. 32). During the tests, all the out-of-plane and torsional deformations of the column and beams are restrained by the out-of-plane braces (Fig. 30, Fig. 31 and Fig. 33).

Table 21 Geometric properties of the test specimens

Specimen	A (mm^2)	I ($10^4 mm^4$)	r (mm)	λ	$\bar{\lambda}$
1-690-1300	2800	673.3	49.0	26.5	0.43
2-960-1300	1724	236.1	37.0	35.1	0.59
3-690-2700	2800	673.3	49.0	55.1	0.82
4-960-2700	2800	673.3	49.0	55.1	0.98
5-690-3600	1260	138.7	33.2	108.5	1.20
6-960-3600	1760	274.1	39.5	91.2	1.34
7-690-3600	750	43.1	24.0	150.1	1.47
8-960-3600	1008	58.2	24.0	149.8	1.76

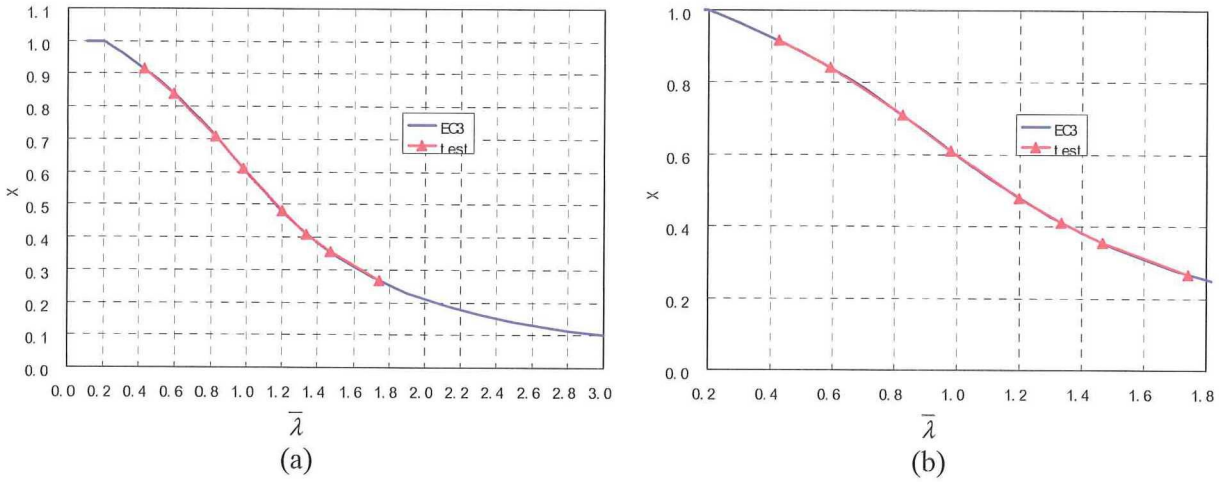

Fig. 29. Distribution of non-dimensional slenderness for all the specimens

The strains of 3 sections are measured as shown in Fig. 30. One is the column mid-height section, and the other two are beam end sections close to the beam-to-column connections. The strain gauge arrangements are shown in Fig. 32 and Table 22.

Table 22 Serial number of the strain gauges

Strain Gauge No.	Strain Gauge Name	Section No.	Strain Gauge No. in section
01	SG1-1	1	01
02	SG1-2	1	02
03	SG1-3	1	03
04	SG1-4	1	04
05	SG1-5	1	05
06	SG1-6	1	06
07	SG1-7	1	07
08	SG1-8	1	08
09	SG1-9	1	09
10	SG2-1	2	01
11	SG2-2	2	02
12	SG2-3	2	03
13	SG2-4	2	04
14	SG2-5	2	05
15	SG2-6	2	06
16	SG2-7	2	07
17	SG2-8	2	08
18	SG2-9	2	09
19	SG2-10	2	10
20	SG2-11	2	11
21	SG2-12	2	12
22	SG2-13	2	13
23	SG3-1	3	01
24	SG3-2	3	02
25	SG3-3	3	03
26	SG3-4	3	04
27	SG3-5	3	05
28	SG3-6	3	06
29	SG3-7	3	07
30	SG3-8	3	08
31	SG3-9	3	09

To exclude the influence of the beam-column joint panel zone, two steel blocks are used to connect the beams and column (Fig. 34). On both beam end supports load cells are used to measure the beam end reaction force.

4.2 Test procedure

The specimens were subjected to a monotonic axial compression force on the column top end which was applied by a 2500kN hydraulic actuator with a maximum piston stroke of ±100 mm. Tests were carried out under displacement control with a constant speed of 0.006 mm/s up to collapse of the specimens.

Acknowledgements

The authors would like to express the sincere gratitude to Mr. Albert Bosman for his excellent work of the experiments. The authors also wish to express appreciation to Mr. Henk Kolstein, Mr. Peter Berkhout, Mr. Arjen van Rhijn, Mr. Edwin Scharp, Mr. Ron Mulder, Mr. John Hermsen, Mr. Kees van Beek.

The friendship and support of Ms. Marijanne Mulder, Prof. Jaap Wardenier and Dr. Addie van der Vegte are very much appreciated. We thank Ms. Anneke Meijer and Ms. Marjo van der Schaaf for the help during the work.

To Marrten Mulder, Nadine Edi Montaruli, Richard Pijpers, Carmen Sandhaas, Nesen Surmeli, Eelke Focke Thank you for your friendship.

Thank Nol Gresnigt, Roland Abspoel and Jan-Willem van de Kuilen for their assistance.

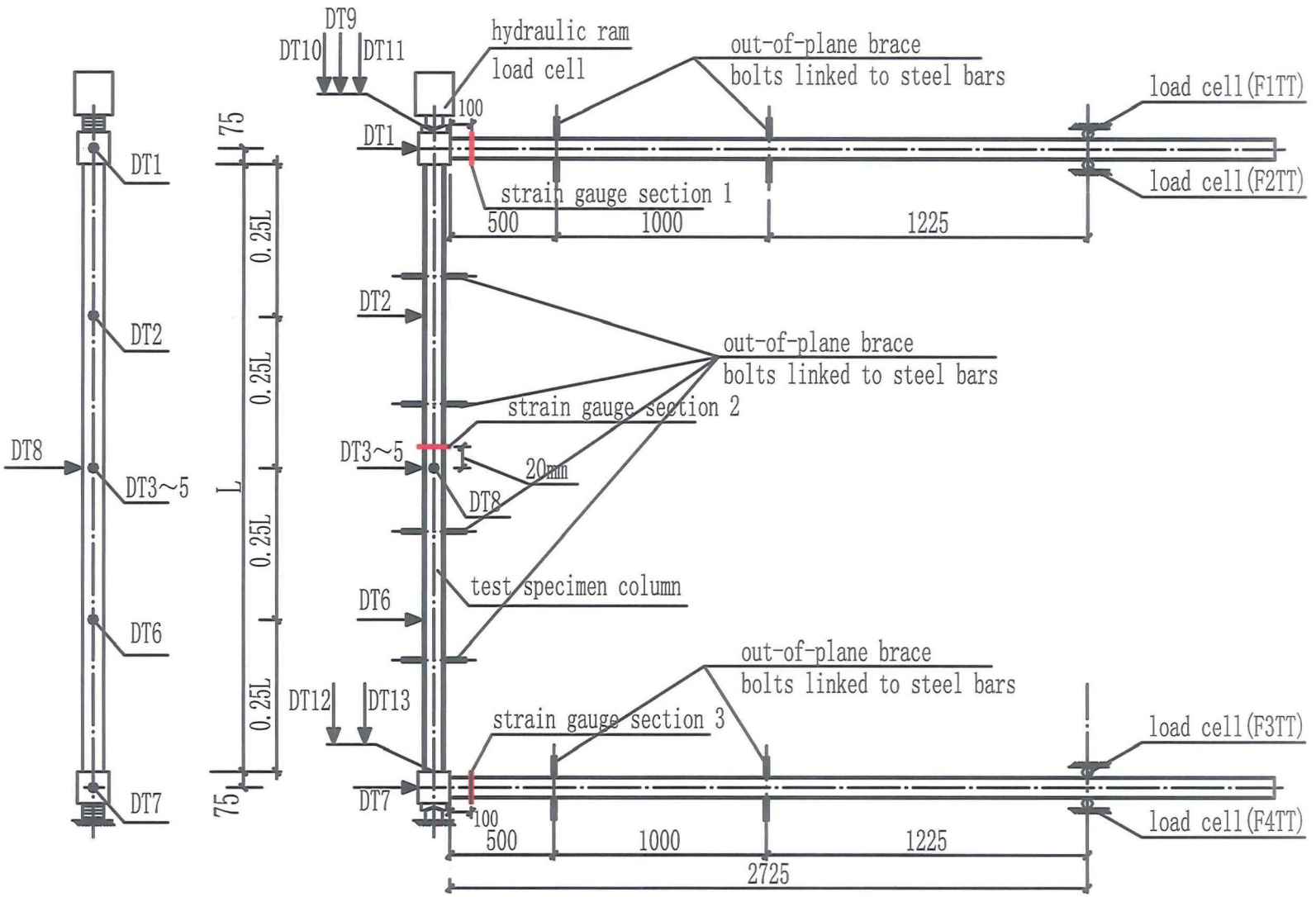

Fig. 30. Test configuration

Fig. 31. Test set-up

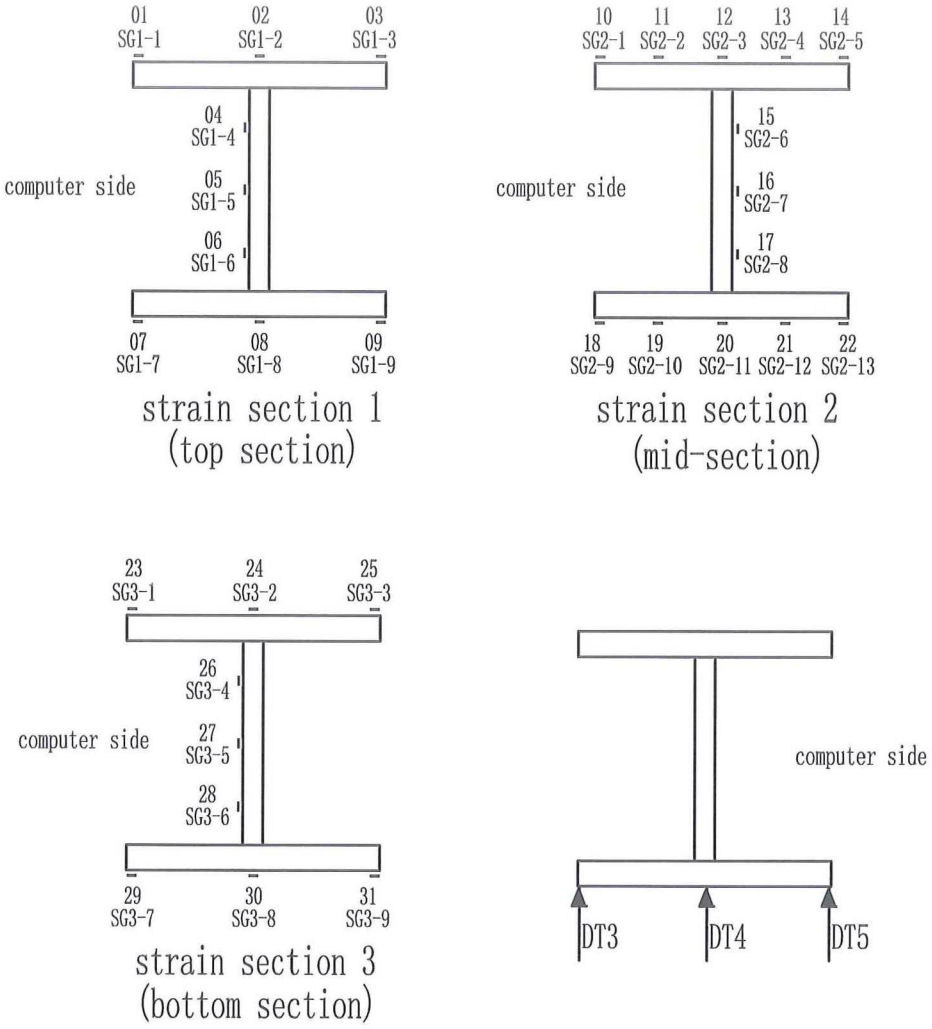

Fig. 32. Strain Gauge Sections

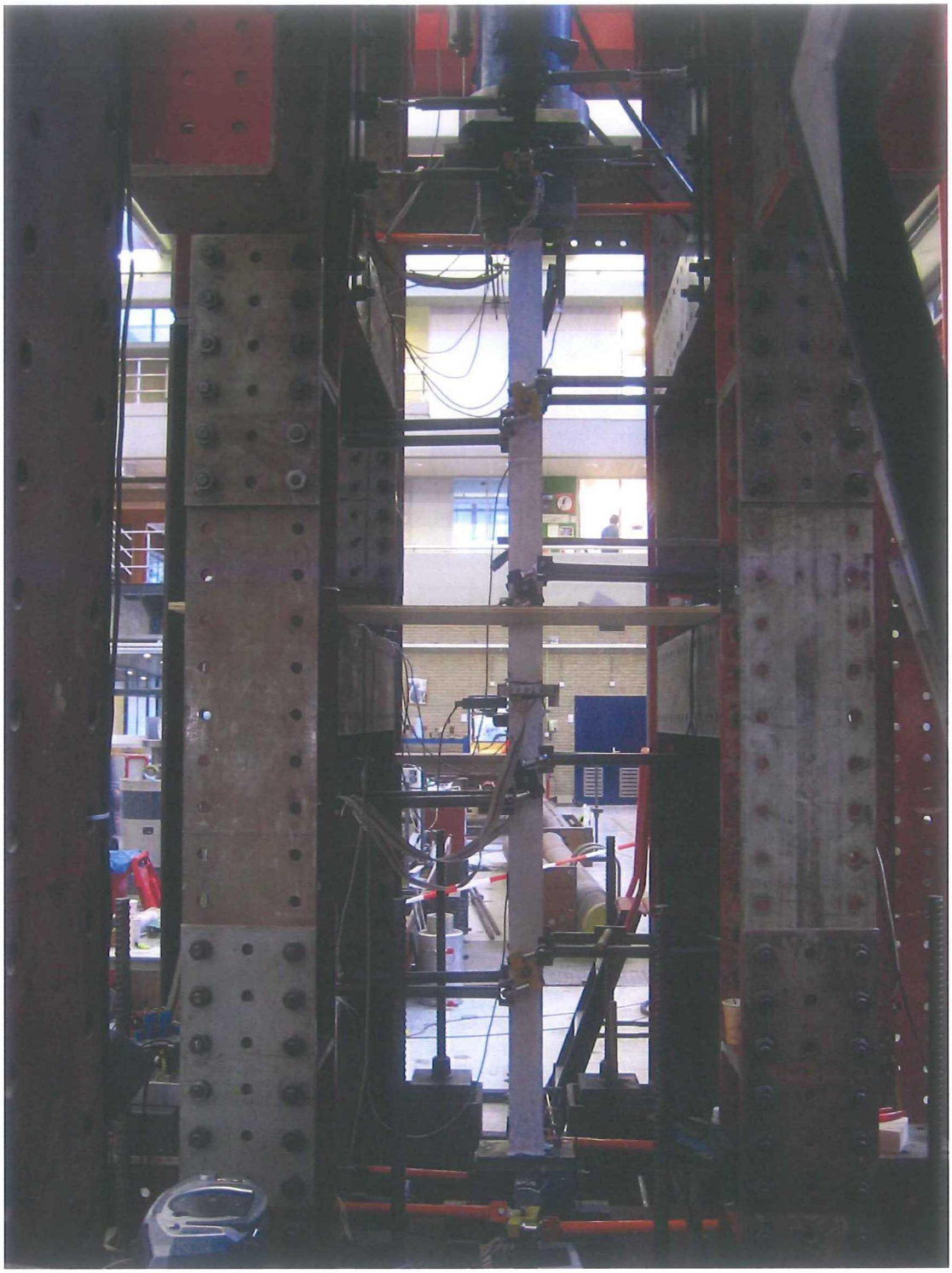

Fig. 33. The arrangement of out-of-plane braces

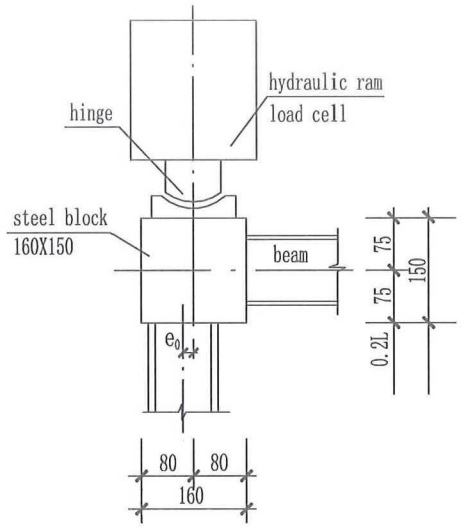

Fig. 34. Column end details

References

[1] International Association for Bridge and Structural Engineering. Use and Application of High-Performance Steels for Steel Structures. Zurich: IABSE, 2005.

[2] Rasmussen K J R , Hancock G J. Tests of high strength steel columns. Journal of Constructional Steel Research, 1995, 34(1): 27-52.

[3] Maquoi R. Some improvements to the buckling design of centrally loaded columns. Structural Stability Research Council, Proceedings of the Annual Meeting, 1982.

[4] CEN : EN 1993-1-1 Eurocode 3 : Design of Steel Structures Part 1.1 General rules and rules for buildings. 2005.

[5] Girão Coelho A.M., Bijlaard, F.S.K. Experimental behaviour of high strength steel end-plate connections. Engineering Structures.(in press)

[6] Gustafsson M. Thickness effect in fatigue of welded extra high strength steel joints. Design and analysis of welded high strength steel structures-Papers presented at a meeting organized in conjunction with the Eighth International Fatigue Congress *FATIGUE 2002* held in Stockholm, Sweden 3-7 June, 2002: 205-224.

[7] Olsson K. E. and Kahonen A. Profitability of high strength steels in fatigue loaded structures. Design and analysis of welded high strength steel structures-Papers presented at a meeting organized in conjunction with the Eighth International Fatigue Congress *FATIGUE 2002* held in Stockholm, Sweden 3-7 June, 2002: 247-276.

[8] Nishino F, Ueda Y, Tall L. Experimental investigation of the buckling of plates with residual stresses. Tests methods for compression members, ASTM special technical publication No. 419, American Society for Testing and Materials, Philadelphia, PA, 1967 : 12-30.

[9] Rasmussen K J R, Hancock G J. Plate slenderness limits for high strength steel sections. Journal of Constructional Steel Research, 1992, 23: 73-96.

[10]McDermott J F. Local plastic buckling of A514 steel members. Journal of the Structural Division, 1969, 95(ST9): 1837-1850.

[11]Clarin M., Lagerqvist O. plate buckling of high strength steel – experimental investigation of welded box sections under compression. 4th European Conference on Steel and Composite Structures: Research – Eurocodes – Practice (Eurosteel 2005). 8-10 June 2005, Maastricht, The Netherlands. Volume 1: 1.4-207 – 1.4-214.

[12]Beg D. and Hladnik L. Slenderness limit of class 3 I cross-sections made of high strength steel, 1996, 38(3): 201-217.

[13]Research School Integral Design of Structures. Research Projects 2006. Delft, The Netherlands.

[14]Usami T , Fukumoto Y. Local and overall buckling of welded box columns. Journal of the

Structural Division, 1982, 108(ST3): 525-542.

[15]Pocock G. High strength steel use in Australia, Japan and the US. The Structural Engineer, 2006, 11: 27-30.

[16]Beg D, Hladnik L. Slenderness limits of class 3 I cross-sections made of high strength steel. Journal of Constructional Steel Research, 1996, 38(3): 201-217.

Annex 1. The input file to define parameters for a typical specimen column (B1150E) model in ANSYS

```
!***********************************************
!Input of All the Parameters
!650 Box section specimens
!***********************************************

!**************File Name*************************
file_name    ='B1150E'  !!define file name

!**************Geometrical Parameters*************************
Web_Height=.0876            !column web net height
Web_Thickness=0.00495       !column web thickness
Weld_size=Web_Thickness     !weld root size
Web_Partitions=18           !segment number of web
Column_Length=1.150         !column length
Col_ele_num=20              !column elements number

!**************Material Parameters*************************
fy=705e6                    !steel yield strength
fu=750e6                    !steel ultimate tensile strength
elastic_modulus=213e9  !elastic modulus of steel,
poisson_ratio=0.3           !Poisson's ratio of steel, 0.3
eu=0.076                    !steel ultimate tensile strain

!**************Loads*************************
col_axial_force=1000000   !column axial force (N)
load_control_factor=0.3   !estimate the column buckling resistance is 0.06*Euler load
ini_geo_imp_factor=0.00183!initial geometric imperfection factor

!***Residual Stresses Distribution Parameters*******
!*web residual stresses values
web_edge_tension=1*fy          !web edge maximum tension residual stress
web_compression_stress=-0.27*fy   !web maximum compression residual stress
web_edge_varying_stress=(1-0.5/(web_edge_tension/(web_edge_tension-
web_compression_stress)))*web_edge_tension   !web edge varying residual stress
```

Annex 2. The input file to generate a typical specimen column (B1150E) section in ANSYS

```
/PREP7
k, 1,-Web_Height/2              , Web_Height/2
k, 2, Web_Height/2              , Web_Height/2
k, 3, Web_Height/2              , -Web_Height/2
k, 4,-Web_Height/2              , -Web_Height/2
k, 5,-Web_Height/2              , Web_Height/2+Web_Thickness
k, 6, Web_Height/2              , Web_Height/2+Web_Thickness
k, 7, Web_Height/2              , -Web_Height/2-Web_Thickness
k, 8,-Web_Height/2              , -Web_Height/2-Web_Thickness
k, 9,-Web_Height/2-Web_Thickness , Web_Height/2
k,10, Web_Height/2+Web_Thickness , Web_Height/2
k,11, Web_Height/2+Web_Thickness , -Web_Height/2
k,12,-Web_Height/2-Web_Thickness , -Web_Height/2

a,1,5,6,2
a,2,10,11,3
a,3,7,8,4
a,4,12,9,1
a,1,9,5
a,2,6,10
a,3,11,7
a,4,8,12

ALLSEL
LSEL,S,LOC,X,0.00001,-0.00001
LSEL,A,LOC,Y,0.00001,-0.00001
CM,Long_line,LINE
LESIZE,Long_line,,,Web_Partitions

ALLSEL
CMSE,U,Long_line
CM,Short_line,LINE
LESIZE,Short_line,,,1

ET,1,PLANE82
ALLSEL
AMESH,ALL

secwrite,Beam_Section,sect,,1
finish
```

Annex 3. The main input file to do the FEA of a typical specimen column (B1150E) in ANSYS

```
parameter_input    !input all the parameters
section_forming    !generate the column section
residual_pattern_01 !generate the residual stresses file
/CLEAR,NOSTART     !clear the database to create the FE model
parameter_input    !input all the parameters agian

/PREP7
!!*****************************************************
!!*****************Element Type************************
ET,1,BEAM188
KEYOPT,1,8,3
SECTYPE,1,BEAM,MESH,
SECOFFSET,CENT,,,
SECREAD,'Beam_Section','sect',' ',MESH
!SECCONTROL,1e10, ,1e10,0,     !neglect the shear deformation

!!*****************************************************
!!*****************Material Behaviour******************
MPTEMP,,,,,,,,
MPTEMP,1,0
MPDATA,EX,1,,elastic_modulus   !elastic modulus of steel,
MPDATA,PRXY,1,,poisson_ratio   !Poisson's ratio of steel, 0.3
TB,MKIN,1,,,0
TBMODIF,1,2,fy/elastic_modulus !steel yield strain
TBMODIF,1,3,eu              !steel ultimate tensile strain
TBMODIF,2,2,fy              !steel yield strength
TBMODIF,2,3,fu              !steel ultimate tensile strength

!!*****************************************************
!!*****************Create Model************************
!!generate column nodes
N,1
N,Col_ele_num+1,,Column_Length
Fill
N,Col_ele_num+2,Column_Length/2,Column_Length/2,  !column element orientation node
!generate column elements
*do,i,1,Col_ele_num
 e,i,i+1,Col_ele_num+2
*enddo

ALLSEL,ALL
/ESHAPE,1.0
eplot

!!*****************************************************
!!*****************First, Static Analysis**************
```

```
/SOLU
antype,static,
pstres,on

!!!displacement restraints
D,ALL,UX
D,col_ele_num+1, UZ,
D,1, UY,
D,1, UZ,
D,ALL,ROTY

F,col_ele_num+1,FY,-(col_axial_force ) !!!column axial force

solve
save
finish

!!*****************************************************
!!!********Secondely, Eigenvalue Buckling Analysis***********
/SOLU
antype,buckle,
bucopt,subsp,1  !!!use Subspace iteration solution method, extract 3 modes
!bucopt,LANB,2  !!!use Block Lanczos solution method, extract 2 modes
mxpand,,,,yes  !!!specify expansion pass options
outpr,nsol,all  !!!only output nodal DOF solution
solve
finish
save

!!*****************************************************************
!!***Thirdly, Calculate Buckling Resistance of Column with ***********
!!***Initial Geometric Imperfection and Residual Stresses***********
/POST1
SET,FIRST
NSORT,U,Z              !sort all the nodes by the z-direction displacement
                  !as the column will buckle about the weak axis
*GET,Z_disp_01,SORT, ,MAX  !get the maximum of the node z-direction displacement
*GET,Z_disp_02,SORT, ,MIN  !get the maximum of the node x-direction displacement
Z_disp_02=ABS(Z_disp_02)
*IF,Z_disp_01,LT,Z_disp_02,THEN
Z_disp_01=Z_disp_02
*ENDIF

*GET,load_factor,MODE,1,FREQ    !get the eigenvalue buckling load factor
col_axial_force=col_axial_force*load_factor*load_control_factor !calculate the applied
load needed

/prep7
!!apply initial geometrical imperfection
ini_geo_imp=ini_geo_imp_factor*Column_Length
```

```
UPGEOM,ini_geo_imp/Z_disp_01,1,1,file_name,'rst',' '

!!Solve the column buckling resitance
FINISH
/SOLU
F,Col_ele_num+1,FY,-(col_axial_force )  !!!apply the needed column axial load
!!!apply the residual stresses
ISFILE,READ,RESIDUAL,ISI, ,1
!ISFILE,LIST,1, ,

ANTYPE,STATIC
NLGEOM,1
NSUBST,20,0,0
OUTRES,ALL,1
ARCLEN,1,0,0
AUTOTS,-1
SOLVE
save
```

Annex 4. The input file to create the residual stress file for a typical specimen column (B1150E) model in ANSYS

```
!*****************************************************
*DEL,,_PRM
/PREP7
*DIM,_Residual_Stress,,304,6

web_edge_tension=1*fy          !web edge maximum tension residual stress
web_compression_stress=-0.27*fy  !web maximum compression residual stress
web_edge_varying_stress=(1-0.5/(web_edge_tension/(web_edge_tension-
web_compression_stress)))*web_edge_tension  !web edge varying residual stress

!generate the residual stress values for all the integration
points**********************************
*DO,I,1,4
  _Residual_Stress(I,1)=web_edge_tension        !tension residual stress in the top left
web edge
*ENDDO

*DO,I,5,8
  _Residual_Stress(I,1)=web_edge_varying_stress !varying residual stress in the top left
web edge
*ENDDO

*DO,I,9,64
  _Residual_Stress(I,1)=web_compression_stress  !compression residual stress in the
top web center
*ENDDO

*DO,I,65,68
  _Residual_Stress(I,1)=web_edge_varying_stress !varying residual stress in the top
right web edge
*ENDDO

*DO,I,69,76
  _Residual_Stress(I,1)=web_edge_tension        !tension residual stress in the top right
two web edges
*ENDDO

*DO,I,77,80
  _Residual_Stress(I,1)=web_edge_varying_stress !varying residual stress in the right
top web edge
*ENDDO

*DO,I,81,136
  _Residual_Stress(I,1)=web_compression_stress  !compression residual stress in the
right web center
*ENDDO
```

```
*DO,I,137,140
  _Residual_Stress(I,1)=web_edge_varying_stress !varying residual stress in the right bottom web edge
*ENDDO

*DO,I,141,148
  _Residual_Stress(I,1)=web_edge_tension        !tension residual stress in the bottom right two web edges
*ENDDO

*DO,I,149,152
  _Residual_Stress(I,1)=web_edge_varying_stress !varying residual stress in the bottom right web edge
*ENDDO

*DO,I,153,208
  _Residual_Stress(I,1)=web_compression_stress  !compression residual stress in the bottom web center
*ENDDO

*DO,I,209,212
  _Residual_Stress(I,1)=web_edge_varying_stress !varying residual stress in the bottom left web edge
*ENDDO

*DO,I,213,220
  _Residual_Stress(I,1)=web_edge_tension        !tension residual stress in the bottom left two web edges
*ENDDO

*DO,I,221,224
  _Residual_Stress(I,1)=web_edge_varying_stress !varying residual stress in the left bottom web edge
*ENDDO

*DO,I,225,280
  _Residual_Stress(I,1)=web_compression_stress  !compression residual stress in the left web center
*ENDDO

*DO,I,281,284
  _Residual_Stress(I,1)=web_edge_varying_stress !varying residual stress in the left top web edge
*ENDDO

*DO,I,285,304
  _Residual_Stress(I,1)=web_edge_tension        !tension residual stress in the top left web edges and all the welds
*ENDDO
```

```
!*****************************************************************
*CFOPEN,RESIDUAL,ISI,,

*DO,II,1,Col_ele_num
   *VWRITE,'EIS',',',II
   (A3,A1,F15.0)
   *DO,JJ,1,1
   *VWRITE,_Residual_Stress(JJ,1),_Residual_Stress(JJ,2),_Residual_Stress(JJ,3),_Re
sidual_Stress(JJ,4),_Residual_Stress(JJ,5),_Residual_Stress(JJ,6)
   (6F15.2)
   *ENDDO
*ENDDO
*CFCLOS
finish
```

Annex 5. The distribution of the integration points and the division nodes of the specimen column sections in the FEA models

1 Sections of group 1 specimens

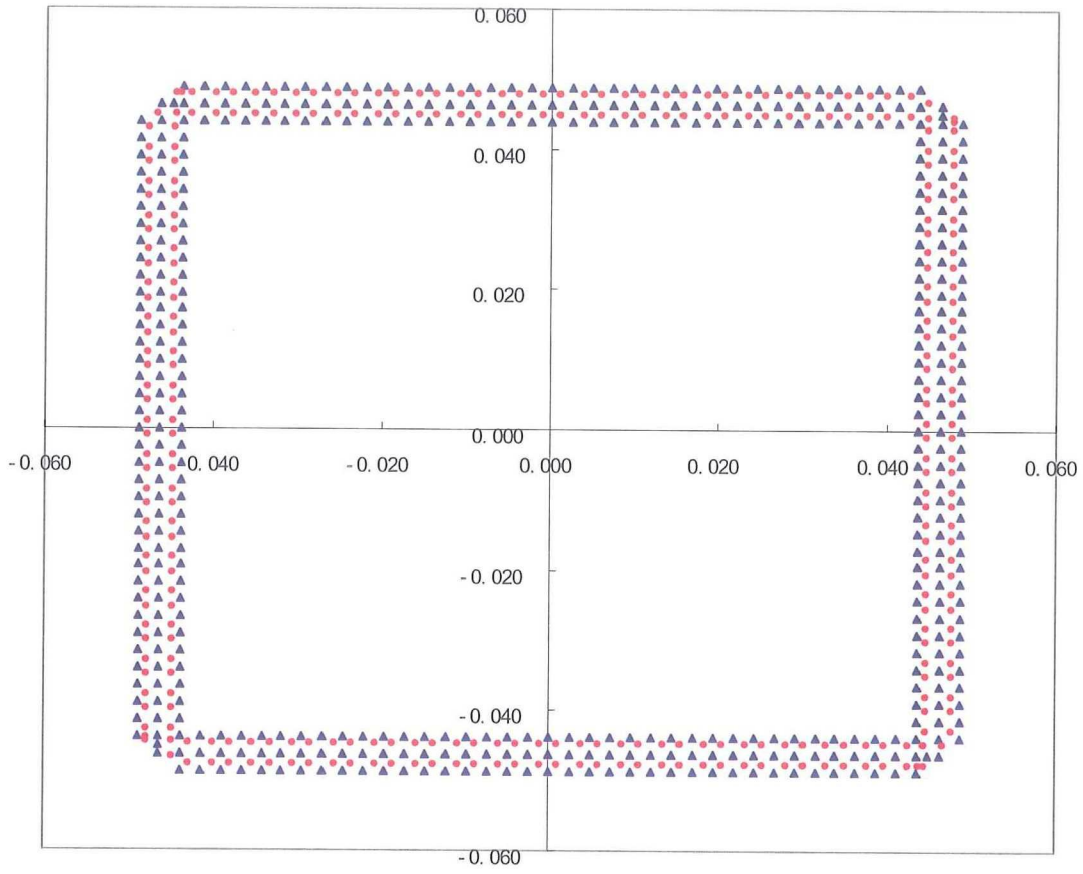

2 Rectangular section of group 2 specimens

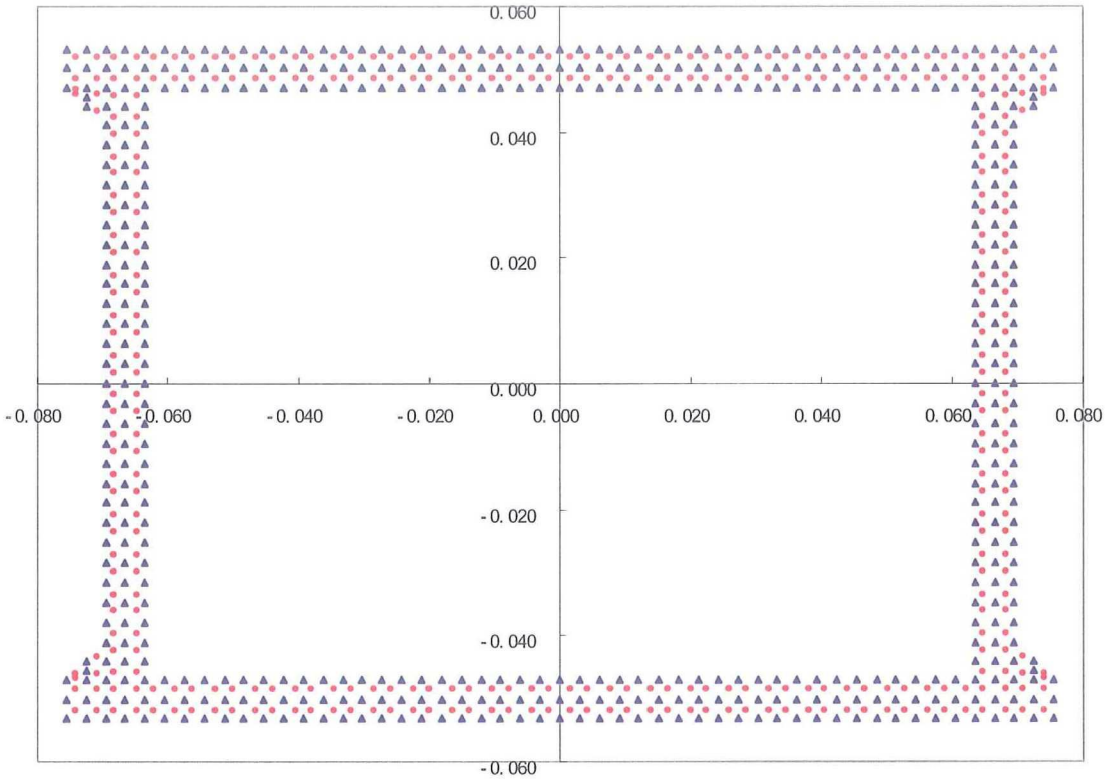

3 Square section of group 2 specimens

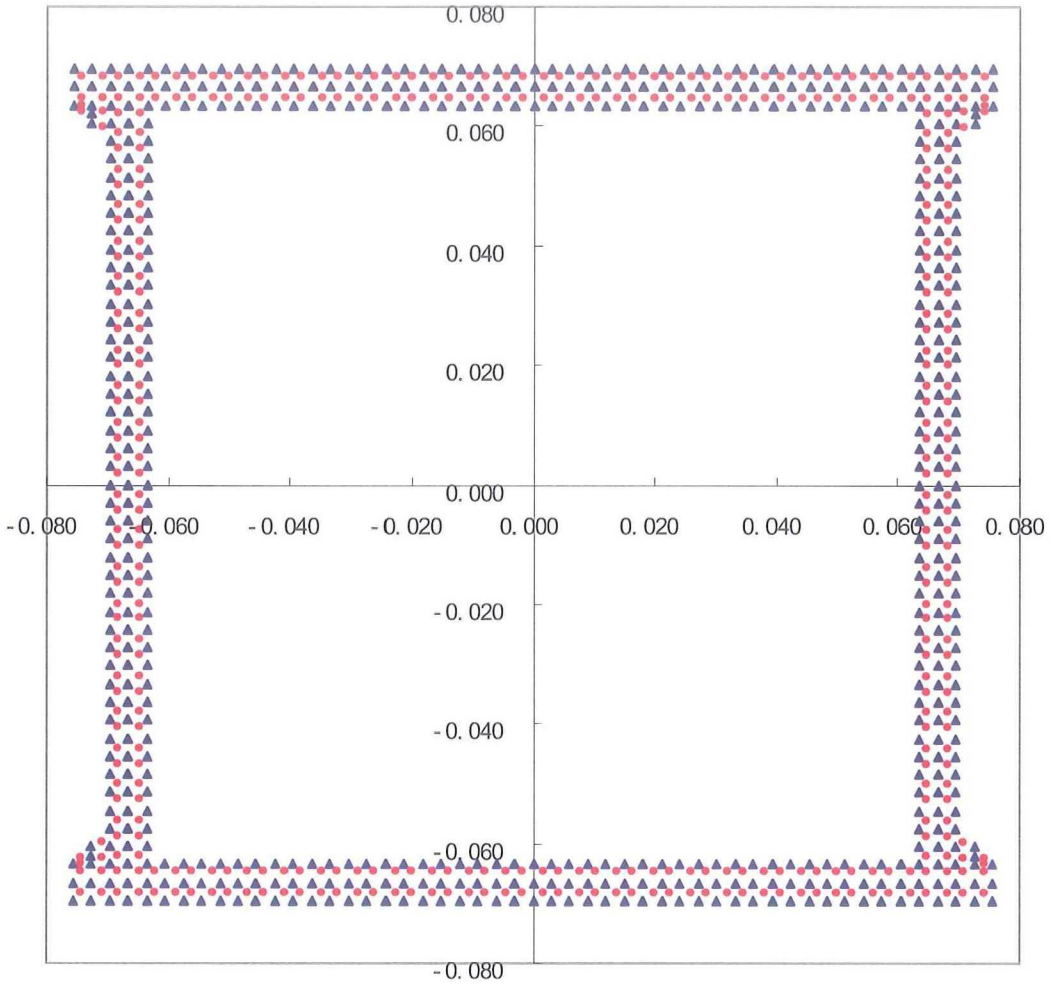

4 Sections of group 3 specimens